Effects of Trace Elements on the Properties of Copper from First-principles Calculations

Effects of Trace Elements on the Properties of Copper from First-principles Calculations

Mingjun Zhong[1], Cheng Peng[1], Fuxiang Huang[1, *], Shuang Liang[1], Baoan Wu[2], Huiyi Tang[2] and Weifan Luo[2]

[1]School of Materials Science & Engineering, Chongqing University of Technology, Chongqing, China
[2]Chongqing materials research institute co., LTD, Chongqing, China

*Corresponding author e-mail: hfx@cqut.edu.cn

Abstract. The effects of X elements (Ag, Ni, Si, Zr, Mg, Al and Zn) doping with amount of 0.926 at% on the structural, mechanical and thermodynamic properties, as well as the electrical properties of Cu were calculated systematically using a first-principles density functional theory (DFT). The calculated formation enthalpy and binding energy indicate that all the $Cu_{107}X$ alloys can be formed and are thermodynamic stable. The B/G values of Cu dilute solutions are between 2.1 and 3.1, both are greater than 1.75, the Poisson's ratios ν are between 0.295 and 0.355, which means that all of $Cu_{107}X$ are plastic materials. $Cu_{107}Si$ and $Cu_{107}Zn$ had the larger Vickers hardness, the value of which were 6.18GPa, 5.97GPa, respectively. By means of molecular dynamics and the Kubo-Green-Wood formula, the electrical conductivities of Cu_{108} and $Cu_{107}X$ were calculated, the results show that all elements doping will reduce the conductivity of Cu, and the conductivity of $Cu_{107}Ag$ in $Cu_{107}X$ alloys is the largest, and its value is $3.56*10^7$S/m.

1. Introduction

Copper and copper alloys have been widely used in light industry, machinery manufacturing, building industry, defense industry and other fields in recent years, especially in the electronic industry, because of its popular price, good electrical and thermal conductivity [1, 2]. Actually, with the development of electronic information industry, more and more requirements are put forward for copper and copper alloy materials, in especially, high strength and high conductivity [3, 4]. High strength and high conductivity of copper alloys are contradictory. As a result, how to improve the strength of copper alloys and control the decrease of its conductivity within a certain range is the key to the research of copper alloys [5]. For copper and copper alloys, strength and conductivity are both influenced by the element doping directly which causes the microstructural changes [6-9]. So, it is valuable to improve the comprehensive properties of copper alloys by regulating and controlling the kinds and amounts of elements. Until now, many different grades of copper alloy have been developed to meet the production needs, in some special industries, such as copper alloys as a new functional material for bonding wires, the amount of experimentations required for research and development is large, and it takes a lot of time and money, and there are few studies to calculate the performance of the simulated copper alloy. Therefore, theoretical prediction for the effects of more alloying additions of Cu can provide essential

guidance in identifying materials with comprehensive properties, and also reduce development cycle and research costs of Cu alloys used as conductive materials.

First-principles calculation based on density functional theory (DFT) is a novel method for micro-investigation at the atomic scale, which is usually used to research the physical properties of solid phases, and the results are widely recognized. In this work, trace elements X (Ag, Ni, Zr, Si, Zn, Mg, Al) were doped into copper, the comprehensive properties of copper alloys were calculated and the essential reasons were explained.

2. Calculation details and crystal structures

The first-principles calculation was carried out by using Cambridge Sequential Total Energy Package (CASTEP) program by constructing a solid solution model with Cu as solvent and X (Ag, Ni, Zr, Si, Zn, Mg, Al) as the solute. The optimized stability structure is calculated for thermodynamic properties, mechanical properties, and electrical properties.

2.1. Calculation details

In the calculation process, the Perdew-Burke-Emzerhof (PBE) potential function in generalized gradient approximation (GGA) is used to process the electron exchange correlation energy part [10, 11]. The accuracy is set to 5.0×10^{-7}eV/atom. After a series of tests, the Brillouin zone integral is selected as Monkhorst Pack [12] 4 × 4 × 4 k-point grid, and the plane wave truncation can be set to 450eV. The geometry of the crystal structure was optimized using the Brodyden-Fletcher-Goldfarb-Shanno (BFGS) minimization method [13]. The convergence accuracy of the total energy is 5.0×10^{-6}eV/atom, the average atomic force is less than 0.1eV/nm, the tolerance offset is less than 5.0×10^{-7}nm, and the maximum stress deviation is 0.02GPa.

2.1.1. Thermodynamic properties. In order to study the thermodynamic stability of Cu107X alloys, the formation enthalpies and binding energies of the alloys were calculated. The formation enthalpy and the binding energy are expressed as ΔH_f and ΔE_{coh}, they are calculated as Eq. (1, 2) [14]:

$$\Delta H_f = \frac{E_{tot}^{Cu_aX_b} - aE_{solid}^{Cu} - bE_{solid}^{X}}{a+b} \tag{1}$$

$$\Delta E_{coh} = \frac{E_{tot}^{Cu_aX_b} - aE_{atom}^{Cu} - bE_{atom}^{X}}{a+b} \tag{2}$$

2.1.2. Elastic constants and mechanical properties. Single-crystal elastic constant Cij, for cubic crystal system, the mechanical stability criteria can be expressed as Eq. (3) [15]:

$$C_{11}>0,\quad C_{12}>0,\quad C_{44}>0,\quad C_{11}-C_{12}>0,\quad C_{11}+2C_{12}>0 \tag{3}$$

Voigt-Reuss-Hill approximation [16] which can be calculated according to Eqs. (4) and (5):

$$B_H = \frac{C_{11}+2C_{12}}{3} \tag{4}$$

$$G_H = \frac{C_{11}-C_{12}+3C_{44}}{10} + \frac{5(C_{11}-C_{12})C_{44}}{6(C_{11}-C_{12})+8C_{44}} \tag{5}$$

The Young's modulus E and Poisson's ratio ν of the polycrystalline material can be obtained by Eqs. (6) and (7) [17]:

$$E = \frac{9BG}{3B+G} \tag{6}$$

$$\nu = \frac{3\mathrm{B}-2\mathrm{G}}{2(3\mathrm{B}+\mathrm{G})} \tag{7}$$

The hardness of a material can usually be predicted according to the semi-empirical formula by Eq. (8) [18]:

$$H\mathrm{v} = \frac{1-2\nu}{6(1+\nu)}E \tag{8}$$

2.1.3. Electrical properties. The electrical properties are obtained using the Kubo-Green-wood formulation which leads to the real part of the electrical conductivity [19, 20]:

$$\sigma_1(K,\omega) = \frac{2\pi \mathrm{e}^2\hbar^2}{3\mathrm{m}^2\omega\Omega}\sum_{\mathrm{j}=1}^{\mathrm{N}}\sum_{\mathrm{i}=1}^{\mathrm{N}}\sum_{\alpha=1}^{3}\left[F(\in_{\mathrm{i},K})-F(\in_{\mathrm{j},K})\right]\times\left|\langle\psi_{\mathrm{j},K}|\nabla_\alpha|\psi_{\mathrm{i},K}\rangle\right|^2\delta(\in_{j,K}-\in_{\mathrm{i},K}-\hbar\omega) \tag{9}$$

2.2. Crystal structures

Cu belongs to face-centered cubic structure, with a space group of Fm-3m, a lattice constant of a=b=c=3.6146 Å, and α=β=γ=90° [21]. In this work, simulating the doping of trace X (Ag, Ni, Zr, Si, Zn, Mg, Al) atoms in Cu by constructing a 3 × 3 × 3 supercell model containing 108 atoms, when pure copper Cu_{108} is replaced by 1 X atom After that, the doping alloy is represented by $Cu_{107}X$, wherein the X content is 0.926 at%, the crystal structure is shown in Fig. 1.

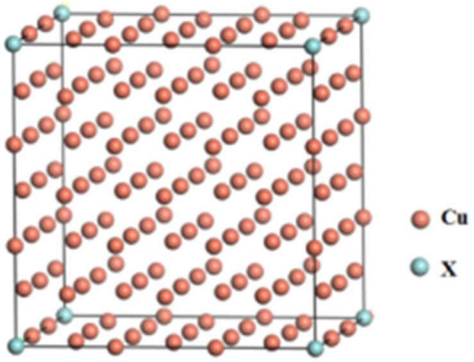

Figure 1. $Cu_{107}X$ solid solution model

3. Results and discussions

3.1. Structural properties

In the constructed solid solution structure model, the incorporation of solute atom X causes lattice distortion of the original Cu structure, which in turn changes the lattice parameters. The optimized lattice parameters and the corresponding atomic radius, together with the available experimental lattice parameters of Cu-X alloy at normal temperature are listed in Table 1. For Cu_{108}, the lattice parameters obtained after optimization is 3.6364Å, which is close to the experimental value of 3.6074Å in [22], the deviation is only 0.8%, and the lattice parameters calculated by Grabowski [23] is 3.658 Å. Comparing with the literatures [22], calculated lattice parameters of $Cu_{107}X$ (Ni, Zn, Mg) are larger than the

experimental values of Cu-1.74at%Ni, Cu-1.66at%Zn, Cu-1.11at%Mg, due to the GGA functional processing exchange correlation energy used in the calculation, however the calculated value is consistent with the experimental value change trend, and the maximum deviation of less than 0.9%, which indicating the excellent accuracy of this work. References are cited in the text just by square brackets [1]. Two or more references at a time may be put in one set of brackets [3, 4]. The references are to be numbered in the order in which they are cited in the text and are to be listed at the end of the contribution under heading references, see our example below.

Table 1. Lattice parameters of $Cu_{107}X$ along with the available experimental data and atomic radius

Phase	Lattice parameters (Å)	Experimental lattice parameters (Å)[22]	Difference of lattice parameters (%)	Atomic radius (Å)[24]
Cu_{108}	3.6364	3.6074	0.8	1.278
$Cu_{107}Ag$	3.6444	-	-	1.444
$Cu_{107}Ni$	3.6355	3.6065	0.8	1.246
$Cu_{107}Zr$	3.6480	-	-	1.60
$Cu_{107}Si$	3.5438	-	-	1.11
$Cu_{107}Zn$	3.6394	3.6125	0.7	1.332
$Cu_{107}Mg$	3.6427	3.6227	0.5	1.60
$Cu_{107}Al$	3.6396	-	-	1.431

According to Hume-Rothery 's law, the solid solution lattice parameter mainly depends on several factors: atom size, crystal structure and solvent atom concentration. Since the doping amount is uniformly 0.926 at%, the influence of the solvent atom concentration can be ignored. It's worth noting that the lattice parameter of $Cu_{107}X$ (Ni, Al, Ag) alloys increase with the radius of X atom which is because Cu has the same crystal structure as Ni, Al, and Ag, and the lattice parameter is almost only affected by the radius of the solvent atom. Zn, Mg, Si and Cu have different crystal structures, considering the influence of atomic radius and crystal structure, Si doping reduces the lattice parameter, and Zn, Cr and Mg doping make the lattice parameter increase. $Cu_{107}Si$ has the smallest lattice parameter (3.5438Å) and $Cu_{107}Zr$ has the largest lattice parameter (3.6480Å) of all calculated $Cu_{107}X$ alloys. Please keep a second copy of your manuscript in your office. When receiving the paper, we assume that the corresponding authors grant us the copyright to use the paper for the book or journal in question. Should authors use tables or figures from other Publications, they must ask the corresponding publishers to grant them the right to publish this material in their paper.

3.2. *Thermodynamic stability*

In order to investigate the thermodynamic stabilities of $Cu_{107}X$ alloys, the formation enthalpy and the binding energy were calculated according to Eqs. (1) and (2).

The results of formation enthalpies and the binding energies are listed in Table 2. From it, the binding energy of Cu_{108} is calculated to be -3.6644eV·atom^{-1}, which is only 5% compared with the experimental value of -3.49eV·atom^{-1} [25], showing that the calculation of the formation and binding energies of $Cu_{107}X$ alloy is reliable. And Cu_{108} is a simple substance, and its formation enthalpy is 0 eV·atom^{-1}. The formation enthalpies of the $Cu_{107}X$ alloys formed by doping X atoms is small, indicating that they can all be formed. Among them, $Cu_{107}Si$ has a maximum enthalpy of 3.03×10^{-2} eV·atom^{-1}, $Cu_{107}Al$ and $Cu_{107}Zn$ have smaller enthalpies which are -0.5×10^{-2}eV·atom^{-1} and -0.14×10^{-2} eV·atom^{-1}, so $Cu_{107}Al$ and $Cu_{107}Zn$ are the easiest to produce compared with other alloys, and $Cu_{107}Si$ is not as easy to form as other alloys.

From Table 2, all the calculated results of binding energies are negative, which indicates that the structures of $Cu_{107}X$ alloys are thermodynamic stable. The binding energy of $Cu_{107}X$ increases gradually

with the increasing binding energy of the corresponding metal [22]. However, it's worth noting that $Cu_{107}Si$ and $Cu_{107}Al$ are different, due to their various crystal structure, which indicates that the crystal structure shows the role to influence the binding energy of $Cu_{107}X$ alloys, Si and Cu have different crystal structures, and larger lattice distortion occurs after doping, resulting in a decrease in binding energy, while Al is the opposite. Among all $Cu_{107}X$ alloys, $Cu_{107}Zn$ and $Cu_{107}Mg$ have poor structural stability, and their binding energies are -3.6406 and -3.6441 $eV{\cdot}atom^{-1}$, respectively. The absolute binding energies of $Cu_{107}Ni$, $Cu_{107}Zr$, and $Cu_{107}Al$ alloys are all greater than the absolute value of Cu_{108} binding energy, so their crystal structure stability is higher than that of pure copper, and the $Cu_{107}Zr$ has the best structural stability and its binding energy is -38.88 $eV{\cdot}atom^{-1}$.

Table 2. The calculated results of $Cu_{107}X$ alloys unit cell total energy, formation energy ΔH_f and binding energy ΔE_{coh}, solid atom and isolated atom average energy

Phase	unit cell energy(eV)	solid atom energy(eV)	atom energy(eV)	$\Delta H_f * 10^{-2}$ ($eV{\cdot}atom^{-1}$)	ΔEcoh ($eV{\cdot}atom^{-1}$)
Cu_{108}	-181540.7658	-1680.9330	-1677.2686	0.00	-3.6644
$Cu_{107}Ag$	-183864.2237	-4004.8793	-4002.2053	0.45	-3.6507
$Cu_{107}Ni$	-181222.2390	-1362.5547	-1357.6711	0.14	-3.6743
$Cu_{107}Zr$	-181152.5596	-1293.2194	-1286.3244	0.45	-3.6898
$Cu_{107}Si$	-180027.0434	-170.4862	-165.1458	3.03	-3.6496
$Cu_{107}Zn$	-181897.1781	-2037.1937	-2036.2568	-0.14	-3.6406
$Cu_{107}Mg$	-181550.1349	-1690.3233	-1688.8324	0.02	-3.6441
$Cu_{107}Al$	-179971.2443	-110.8733	-107.1756	-0.50	-3.6697

3.3. Mechanical properties

3.3.1. Elastic constants and elastic properties. The calculated elastic constants and elastic properties for the Cu_{108} and $Cu_{107}X$ alloys are listed in Table 3. As Cu_{108} and $Cu_{107}X$ show cubic structures, their mechanical stability estimate should be followed by Eq. (3). From Table 3, all calculated Cu_{108} and $Cu_{107}X$ alloys are stable. The bulk modulus B, shear modulus G, Young's modulus E were calculated by Eqs. (4) – (6), and the calculated results are listed in Table 3.

From Table 3, the doping of Mg, Zn, Zr, Ag and Al reduces the modulus of the $Cu_{107}X$ alloy to a different extent, only because the metal has a small modulus. And the bulk modulus of $Cu_{107}Ni$ is increased to 136.6GPa, due to the bulk modulus of Ni is larger than that of Cu. The bulk modulus of $Cu_{107}Si$ is significantly increased to 191.8GPa, which becomes the maximum value of the bulk modulus in the $Cu_{107}X$ alloys, since the doping of Si element greatly reduces the lattice constant of Cu_{108}, reducing the lattice volume helps to increase the average force between atoms. The Young's modulus is used to characterize the strength of bonding between atoms and to reflect the amount of bonding between atoms. As shown in Table 3, the Young's modulus and shear modulus of $Cu_{107}X$ alloys are consistent, and the Young's modulus and shear modulus of $Cu_{107}Si$ are relatively large, with values of 169.8GPa and 62.8GPa. The Young's modulus and shear modulus of $Cu_{107}Zn$ and $Cu_{107}Mg$ are relatively large, for cubic crystal, G and E are positively related to the binding energy. At the same time, in engineering, the

Young's modulus is a measure of material stiffness. Therefore, $Cu_{107}Mg$, $Cu_{107}Zn$, and $Cu_{107}Si$ are more rigid than other alloys.

Table 3. Elastic properties of Cu_{108} and $Cu_{107}X$ alloys

Phase	C_{11}	C_{12}	C_{44}	B_H(GPa)	G_H(GPa)	E (GPa)
Cu_{108}	172.0	123.2	78.5	135.5	41.4	113.0
$Cu_{107}Ag$	154.1	109.0	80.3	124.0	48.5	128.6
$Cu_{107}Ni$	153.7	113.7	80.9	136.6	46.5	124.3
$Cu_{107}Zr$	151.7	111.7	73.3	125.0	43.7	117.5
$Cu_{107}Si$	234.8	170.4	98.0	191.8	62.8	169.8
$Cu_{107}Zn$	159.3	109.4	81.0	126.0	50.6	133.9
$Cu_{107}Mg$	158.0	109.1	80.7	125.4	50.1	132.7
$Cu_{107}Al$	161.1	113.6	77.9	129.4	48.5	129.3

3.3.2. Ductility property. In this work, the plastic properties of Cu_{108} and $Cu_{107}X$ alloys were evaluated by the ratio of the volume modulus to the shear modulus B_H/G_H and the Poisson's ratio ν. A large B_H/G_H and ν indicate the trend for plastic property, and the standardized value distinguishes ductile and brittle materials have been evaluated to 1.75 and 0.33 respectively [19]. The calculated ratio of the volume modulus to the shear modulus B_H/G_H and the Poisson's ratio ν of Cu_{108} and $Cu_{107}X$ alloys by Eq. (7) are shown in Fig. 2.

From Fig. 2, the B/G values of $Cu_{107}X$ alloy are between 2.1 and 3.1, both are greater than 1.75. The Poisson's ratios ν are between 0.295 and 0.355, and the Poisson's ratio ν of $Cu_{107}Dy$ is 0.295, that is slightly less than 0.3, except it the Poisson's ratios ν of other $Cu_{107}X$ alloys are all greater than 0.3. And, it is easy to see that the B/G value is consistent with the law and degree of ν value change. In general, the doping of Zn, Mg, and Ag greatly reduced the plasticity of Cu, so the plasticity of $Cu_{107}Ag$, $Cu_{107}Mg$, and $Cu_{107}Zn$ alloys was worse than that of other $Cu_{107}X$ alloys. The doping of the other elements has little effect on the B/G value and Poisson's ratio ν of Cu, the B/G value and Poisson's ratio ν of $Cu_{107}Si$, $Cu_{107}Ni$ and $Cu_{107}Zr$ are higher than 2.8 and 0.34, respectively, which means they still have good plastic property.

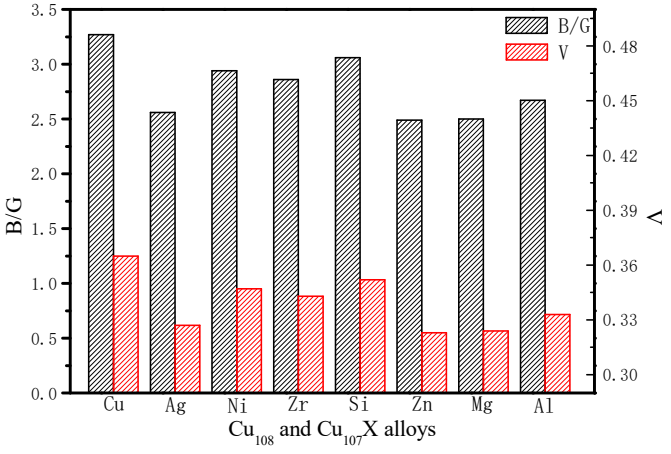

Figure 2. The ratio of the volume modulus to the shear modulus B_H/G_H and the Poisson's ratio ν of Cu_{108} and $Cu_{107}X$ alloys

3.3.3. Hardness. In order to estimate the hardness of Cu_{108} and $Cu_{107}X$ alloys, the Vickers hardness was calculated by Eq. (8), and the results are shown in Fig.3. From the Fig.3, the calculated Vickers hardness of Cu_{108} is 3.73GPa, which is larger than the experimental value of 1.53GPa at room temperature in the literature [26]. This is because the Cu_{108} used in the calculation is a structural model under ideal conditions, and the possible defects of the crystal are not considered, and the bond structure is more stable. Therefore, it is reasonable that the theoretical value is higher than the experimental value. The hardness of $Cu_{107}X$ alloys can be seen to affect the hardness of the alloy: Si>Zn>Mg>Ag>Al>Ni>Zr. For metal materials, the influence on the hardness mainly considers the strength of the metal bond, which related to the atomic radius and the number of valence electrons per unit volume. The smaller the atomic radius of the metal, the smaller the average bond length of the metal bond, the higher the bond strength, and the greater the interaction, the greater the hardness. Therefore, the doping of the Si element greatly increases the hardness of the Cu, and the doping of the Ni element also appropriately increases the hardness of the Cu. The more the number of valence electrons per unit volume, the stronger the metal bond and the greater the hardness. Although the three elements of Zr, Zn and Ag are larger than the radius of Cu atoms, they have more valence electrons than Cu, so the hardness of Cu can be increased to different extents after doping. In addition, the Cu-Mg and Cu-Al bonds are more covalent and have a higher hardness.

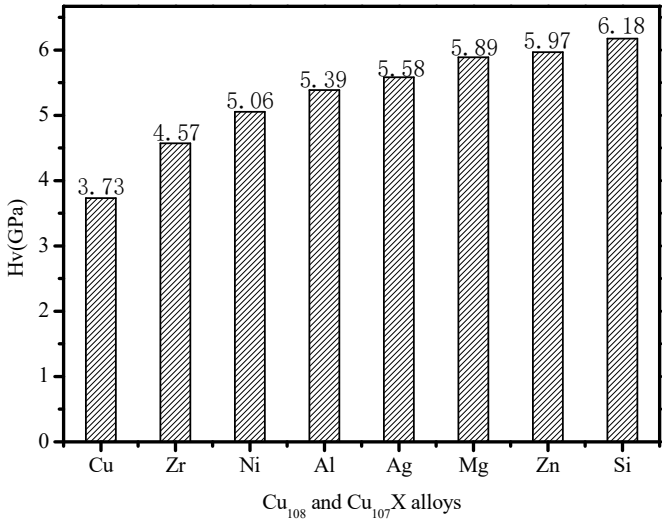

Figure 3. Vickers hardness of Cu_{108} and $Cu_{107}X$ alloys

3.4. Electrical properties

Molecular dynamics was performed on the geometrically optimized Cu_{108} and $Cu_{107}X$ models, including NVE dynamics and NVT dynamics. Then, ten samples were collected for the NVT dynamics trajectory, and the CASTEP optical properties were calculated for the sampling structure. The optical conductivity of Cu_{108} and $Cu_{107}X$ at 300k after calculation using molecular dynamics methods and optical properties is shown in Fig.4.

According to the Kubo-Green-wood formulation, the AC conductivity is calculated, and the conductance at the frequency of 0 is extracted, which is the DC conductivity. The DC conductivity of Cu_{108} and $Cu_{107}X$ alloy is shown in Fig. 5. From the Fig. 5, the calculated conductivity of Cu_{108} is $5.38*10^7$S/m, which is similar to the experimental value of $5.8*10^7$S/m in the literature [27], which verifies the reliability of the calculation. Compared with the conductivity of Cu_{108}, the conductivity of $Cu_{107}X$ are all reduced. The conductivity of $Cu_{107}Al$ and $Cu_{107}Si$ is lower, the values are $2.11*10^7$S/m and $2.31*10^7$S/m respectively. The doping of Ag and Ni has little effect on the conductivity of copper, the conductivity values are $3.56*10^7$S/m and $2.77*10^7$S/m respectively. According to the metal conduction theory, the lattice distortion caused by solid solution atoms enhances the scattering of

electrons, especially the Si dissolved in the alloy has a very strong scattering effect on electrons. Therefore, the conductivity of $Cu_{107}X$ alloys are reduced, and the conductivity of $Cu_{107}Si$ is the smallest.

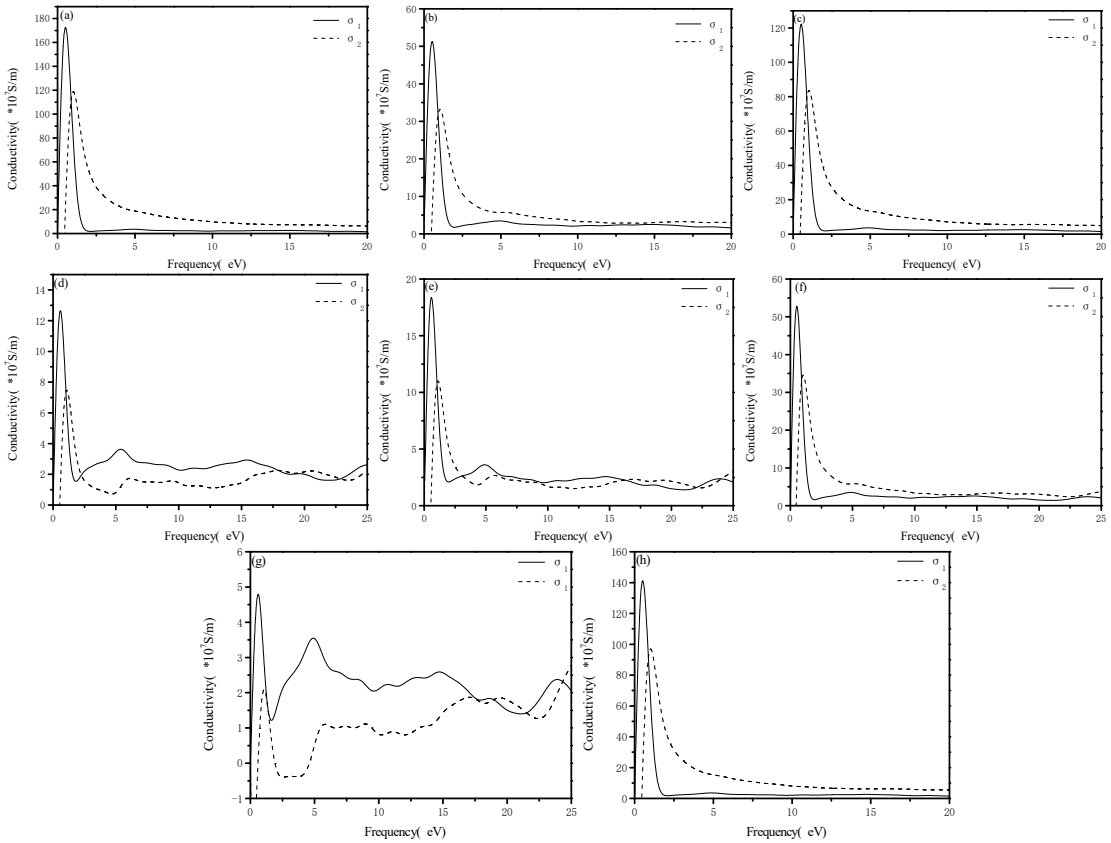

Figure 4. Real and imaginary conductivities of Cu_{108} and $Cu_{107}X$ alloys, (a)Cu_{108}, (b)$Cu_{107}Ag$, (c)$Cu_{107}Ni$, (d)$Cu_{107}Si$, (e)$Cu_{107}Zr$, (f)$Cu_{107}Mg$, (g)$Cu_{107}Al$, (h)$Cu_{107}Zn$

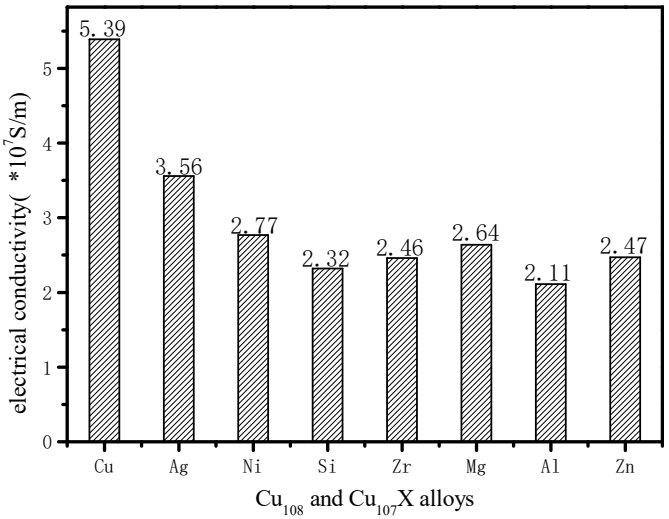

Figure 5. The electrical conductivities of Cu_{108} and $Cu_{107}X$ alloys

4. Conclusion

In this work, the structural, mechanical and thermodynamic properties of Cu_{108} and $Cu_{107}X$ alloys have been investigated systematically by the first principles calculations, and the electrical conductivities

were also investigated. The relevant conclusions are listed as follows: When receiving the paper, we assume that the corresponding authors grant us the copyright to use the paper for the book or journal in question. Should authors use tables or figures from other Publications, they must ask the corresponding publishers to grant them the right to publish this material in their paper.

(1) The lattice constant of $Cu_{107}X$ alloy is mainly affected by the atomic radius of the doping atom X and its crystal structure, and the minimum lattice constant of $Cu_{107}Si$ is 3.5438 Å, the maximum lattice constant of $Cu_{107}Zr$ is 3.6480 Å.

(2) The formation enthalpies of the $Cu_{107}X$ alloys is small, show that all of they can be formed, and all the calculated results of binding energies are negative indicates that the structures of $Cu_{107}X$ alloys are thermodynamic stable.

(3) The bulk modulus of $Cu_{107}Si$ has the largest phantom modulus of 191.8GPa. The Young's modulus of $Cu_{107}X$ alloy is consistent with the change of shear modulus. The B/G and Poisson's ratio ν values of $Cu_{107}X$ alloy are greater than the boundary values of 1.75 and 0.3, indicating that most of the $Cu_{107}X$ alloy has good plasticity. For the $Cu_{107}X$ alloys, the Vickers hardness increases in the following order: Cu_{108}<$Cu_{107}Zr$<$Cu_{107}Ni$<$Cu_{107}Al$<$Cu_{107}Ag$<$Cu_{107}Mg$<$Cu_{107}Zn$<$Cu_{107}Si$, the hardness of $Cu_{107}Si$, $Cu_{107}Zn$ and $Cu_{107}Mg$ are 6.18Gpa, 5.97GPa and 5.89GPa respectively.

(4) The electrical conductivities of Cu_{108} and $Cu_{107}X$ were calculated, the results show that all elements doping will reduce the conductivity of Cu, Ag doping has little effect on the electrical conductivity, the conductivity is $3.56*10^7$S/m, and Si and Al doping have a great influence, the conductivity are $2.32*10^7$S/m and $2.11*10^7$S/m, respectively.

(5) In general, when higher conductivity is preferred, alloying elements such as Ag, Ni, and Mg may be appropriately added. If high mechanical properties are required, alloying elements such as Si, Zn, and Mg may be appropriately added.

Acknowledgments
This work was financially supported by the National Key Research and Development Program of China (Grant No. 2016YFB0402602).

References

[1] S. Q. Wang, Z. Q. Chen, D. L. Peng, et al. A Comprehnve Survey of High Conductivity, High Strength Coppet Based Alloys. Journal of Materials Engineering, 7 (1995) 3-6.
[2] R. R. Liu, H. T. Zhou, X. Zhou, et al. Present Situation and Future Prospect of High-strength and High-conductivity Cu Alloy. Materials Review, 26 (2012) 100-105.
[3] L. Lu, Y. F. Shen, X. H. Chen, et al. Ultrahigh Strength and High Electrical Conductivity in Copper. Science, 304 (2004) 422-426.
[4] S. A. Hosseini, H. D. Manesh. Hosseini S A , Manesh H D . High-strength, high-conductivity ultra-fine grains commercial pure copper produced by ARB process. Materials and Design, 30 (2009) 2911-2918.
[5] C. S. Xie, Q. M. Zhai, W. Q. Xu, et al. Study and Application Development of Strengthening Theory of Copper Alloy with High Strength and High Conductivity.32 (2007) 12-20.
[6] Y. T. Ning, X. H. Zhang, Y. J. Wu. Electrical conductivity of Cu-Ag in situ filamentary composites. Transactions of Nonferrous Metals Society of China, 17 (2007) 378-384.
[7] J. K. Hyung, L. H. Sun. Bending Behavior and Electrical Conductivity of Cu/Ni/Al/Ni/Cu Clad Composite. Materials Science Forum, 909 (2017) 127-132.
[8] S. C. Krishna, K. T. Tharian, B Pant, et al. Microstructure and mechanical properties of Cu-Ag-Zr alloy. Journal of Materials Engineering and Performance, 22 (2013) 3884-3889.
[9] M. Eldrup, B.N. Singh. Influence of composition, heat treatment and neutron irradiation on the electrical conductivity of copper alloys. Journal of Nuclear Materials, 258 (1998) 1022-1027.
[10] J. P. Perdew, K. Burke, M Ernzerhof. Generalized gradient approximation made simple. Physical Review Letters, 77 (1996) 3865-3868.
[11] M. C. Payne, M. P. Teter, D. C. Allan, et al. Iterative minimization techniques for ab initio total-

energy calculations: molecular dynamics and conjugate gradients. Reviews of Modern Physics, 64 (1992) 1045-1097.
[12] D J Chadi. Special points for Brillouin-zone integrations. Physical Review B, 16 (1976) 1748-1749.
[13] T. H. Fischer, J. Almlof. General methods for geometry and wave function optimization. Journal of Physical Chemistry, 96 (1992) 9768-9774.
[14] G. F. Li, S. Q. Lu, X J Dong, et al. Microcosmic mechanism of carbon influencing on $NiTiNb_9$ alloy. Journal of Alloys and Compounds, 524 (2012) 170-176.
[15] J. D. Eshelby. Distortion of a Crystal by Point Imperfections. Journal of Applied Physics, 25 (1954) 255-261.
[16] R. W. Hill. The Elastic Behavior of a Crystalline Aggregate. Proceedings of the Physical Society, 65 (1952) 349-354.
[17] Y. Lu, D. F. Li, B. T. Wang, et al. Electronic structures, mechanical and thermodynamic properties of ThN from first-principles calculations. Journal of Nuclear Materials, 408 (2011) 136-141.
[18] W. C. Hu, Y. Liu, D. J. Li, et al. Structural, anisotropic elastic and electronic properties of Sr-Zn binary system intermetallic compounds: A first-principles study. Computational Materials Science, 99 (2015) 381-389.
[19] S. Mazevet, M. Torrent, V. Recoules, et al. Calculations of the transport properties within the PAW formalism. High Energy Density Physics, 6 (2010) 84-88.
[20] D. W. Zhou, J. F. Song, G. Q. Li. Investigation on the electrical conductivity of fluid potassium under extra conditions. Journal of Nanyang Normal University, 10 (2011) 27-30.
[21] D. Arias, J. P. Abriata. Cu-Zr (copper-zirconium). Journal of Phase Equilibria, 11 (1990) 452-459.
[22] W. B. Pearson. CHAPTER XI-an alphabetical index of work on metals and alloys. A Handbook of Lattice Spacings & Structures of Metals & Alloys, 115 (1958) 319-320.
[23] B. Grabowski, T. Hickel, J. Neugebauer. Ab initio study of the thermodynamic properties of nonmagnetic elementary fcc metals: exchange-correlation-related error bars and chemical trends. Physical Review B, 76 (2007).
[24] J. A. Dean. Lang's handbook of chemistry (thirteenth edition). New York: Mc Graw-Hill Book, 3 (1985).
[25] M. D. Segall, M. J. Probert, C. J. Pickard, et al. First-principles simulation: ideas, illustrations and the CASTEP code. Journal of Physics-condensed Matter, 14 (2002) 2717-2744.
[26] Z Han, B Yao, K Lu. Dynamic recrystallization dominated wear mechanism of nanostructured Cu. Acta Metallurgica sinica, 50 (2014) 238-244.
[27] J. K. Liao, Y. H. Liang, W. W. Li, et al. Silver Alloy Wire Bonding. Electronic Components and Technology Conference (ECTC), 2012 IEEE 62nd.